Flood Impact Assessment on Highway Networks Considering Socioeconomic Vulnerability: Evidence from Harris County

Beixuan Dong[1], Lingzi Wu[2] and Xinming Li[1, *]

[1]Department of Mechanical Engineering, University of Alberta, Canada
[2]Department of Construction Management, University of Washington, USA
beixuan1@ualberta.ca, lingwu@wu.edu, xinming1@ualberta.ca

Abstract –

Flooding can severely disrupt highway networks, causing substantial mobility loss and delayed recovery. Existing studies that quantify flood impacts on transportation networks primarily focus on structural or functional features, largely overlooking the role of socioeconomic vulnerability. Additionally, how socioeconomic vulnerability influences flood impacts and recovery prioritization across traffic-demand groups remains unknown. This study proposed a unified disaster impact index (DII) that integrates predicted traffic performance with surrounding socioeconomic vulnerability to assess flood impacts on highway networks. A graph neural network (GNN)-based model was employed to predict traffic flow and speed under flood conditions, enabling a performance-based evaluation of network disruption. Using Harris County during Hurricane Harvey as a case study, flood impacts on 18 major highways were quantified and compared across high-traffic-, medium-traffic-, and low-traffic-demand groups. Results showed that incorporating socio-economic features did not alter the identification of the most critical highways, but rather reshaped prioritization within the medium-traffic-demand highway group to emphasize highways that serve socially vulnerable communities.

Keywords –

Flood impacts; socioeconomic vulnerability; data analysis; GNN; highway networks

1 Introduction

Flooding is one of the most disruptive natural hazards affecting transportation systems, leading to extensive mobility loss, prolonged traffic delays, and significant socioeconomic consequences [1, 2]. Highway networks, as the backbone of urban mobility and emergency response, are particularly vulnerable when flood overwhelms surface drainage and inundate critical road segments [3]. During Hurricane Harvey, several major highway closures occurred due to flooding, severely constraining regional accessibility and delaying emergency operations [4]. These challenges underscore the growing need to quantify the impacts of disasters on highway networks and identify the most critical roads for effective restoration.

Existing research has examined the impact of flooding on transportation systems from both network structural and functional features. Studies focusing on network structural features typically employ graph-based metrics, such as network efficiency and centrality, to assess changes in connectivity and accessibility. Functional studies, on the other hand, focus on performance degradation such as reduced traffic flow, increased travel time, and loss of capacity to assess the severity of disruptions. However, most existing studies fail to consider the socioeconomic aspects of surrounding communities, limiting the practicality of disaster impacts on transportation networks' recovery.

Recent research has begun to incorporate socioeconomic vulnerability into disaster planning and assessment, recognizing that communities with higher vulnerability tend to face longer recovery times and weaker resilience [5]. These studies have assessed disaster impacts on different regions by AHP [6] and prioritized the recovery of small bridge and road networks considering socioeconomic vulnerability [7]. However, there are two main gaps. First, socioeconomic vulnerability is not integrated with actual functional performance, rendering it static and failing to quantify disaster impacts with a dynamic nature. Second, how socioeconomic vulnerability influences flood impacts and recovery prioritization across traffic-demand groups remains unknown.

To address the research gaps, this study quantified flood impacts integrating network structural, functional, and socioeconomic features on highway networks and explored how socioeconomic vulnerability influences the restoration priorities of different traffic demand highway groups. We developed a disaster impact indicator (DII) that integrates predicted traffic performance from a graph neural network-multi-layer perceptron (GNN-MLP) model with socioeconomic vulnerability of surrounding communities. Using Harris County during Hurricane Harvey as the case study, we quantified flood impacts on 18 highways and examined how integrating social vulnerability can shift recovery priorities across high-traffic-, medium-traffic-, and low-traffic-demand highway groups. The contributions of this study are (1) developing a unified DII that captures network structural, functional, and socioeconomic features to assess flood impacts; (2) investigating how socioeconomic vulnerability influences recovery prioritization across traffic-demand groups.

The remainder of this paper is organized as follows. Section 2 reviews related work on disaster impact assessment for transportation networks. Section 3 introduces the methodology, including the construction of DII. Section 4 presents the case study, results, and discusses key findings. Section 5 concludes with implications for transportation disaster management.

2 Literature Review

This section introduces previous research on disaster impact assessment for transportation networks, focusing on the input features used in these studies (subsection 2.1). We then summarized their input features, strengths, and limitations in Table 1, and finally articulated research gaps and our research objectives (subsection 2.2).

2.1 Disaster Impact Assessment for Transportation Networks

Existing studies on the impacts of disasters on transportation networks have focused on the structural and functional features of these networks. Studies focusing on network structural features typically rely on network topology and connectivity. These studies have been applied to identify urban roads most affected by flash floods [8] and detect system-critical routes under terrorist attacks and volcanic eruptions [9]. However, these methods are simple and intuitive as they directly link the intensity of physical hazard to network vulnerability. Furthermore, they tend to have low fidelity as they ignore dynamic traffic conditions and fail to reflect the broader impact on surrounding communities.

Studies focusing on functional features typically use traffic speed [10], and traffic flow [11, 12] to quantify functional degradation of transportation networks under disaster conditions. These methods provide more quantitative and operationally meaningful estimates of network performance loss. However, they largely overlook the social aspects of transportation systems, treating road segments as isolated infrastructure elements without considering the vulnerable communities they serve.

A small number of studies have attempted to integrate network structural and functional features. They highlight network vulnerabilities across different hazard types and provide a more comprehensive view of operational disruptions [12]. Despite this progress, they still fail to incorporate the influence of socio-economic features from surrounding communities.

More recently, several studies have incorporated socioeconomic features into disaster assessment frameworks. One work has proposed a decision-making framework for transportation recovery planning that recognizes the importance of socioeconomic features [5]. Other studies have developed decision-support tools, such as an AHP-based framework [6], to assess regional earthquake risks considering socio-economic features. However, these studies fail to include real-time assessment, focusing on a macro-level regional risk assessment rather than the road-level assessment. Therefore, Merschman et al. [7] proposed a post-disaster bridge repair framework that incorporates social vulnerability to identify the most resilient recovery strategy. Although they have assessed the resilience for each bridge repair sequence, they did not explore how socio-economic features affect the impact of floods on roads with different travel demands.

Table 1 Representative studies on disaster impact assessments for transportation networks

Ref.	Input features	Strength	Limitation
[8]	Network structural features	Simple, intuitive; directly relates hazard intensity to risk	Low-fidelity; ignores dynamic traffic and impacts to surrounding communities
[10]	Functional features	Provides quantitative estimates of functional performance	Ignores impacts to surrounding communities
[12]	Network structural and functional features	Highlights structural vulnerabilities, applicable to various hazards	Ignores impacts on surrounding communities
[5]	Network structural, functional, and socio-economic features	Provide a decision-making framework for disaster recovery planning	There is no quantitative analysis of the influence of socio-economic

			features
[6]	Physical and socio-economic features	Provide a decision support tool for disaster assessing earthquake risk in different regions	There was no real-time assessment, nor was there an assessment at the road segment level
[7]	Network structural, functional, and socio-economic features	Propose a post-disaster bridge repair planning framework considering social vulnerablity	The selection process for the 8 social vulnerability factors used to construct SVI was subjective.
Our study	**Network structural features, functional features, and socio-economic features**	**Propose a unified disaster impact indicator that quantifies flood impacts**	**Since CDC statistics are collected once a year, social features are not dynamic**

2.2 Research Gaps and Objectives

In summary, there are two main research gaps. First, existing studies lack quantitative and real-time assessments of disaster impacts that integrate socio-economic and dynamic traffic performance. This limitation reduces the reliability of these methods for time-sensitive decision-making during emergency response and recovery planning. Second, although the importance of socioeconomic vulnerability has been increasingly recognized, its role in influencing flood impacts on transportation networks with different travel demand levels remains insufficiently explored. As a result, recovery strategies derived from existing methods may unintentionally fail to prioritize roads that are critical for socially vulnerable communities.

To fill these gaps, this study developed a unified indicator that integrates predicted traffic performance with surrounding socioeconomic vulnerability to assess the flood impacts and support recovery planning. Specifically, we developed a DII that integrates predicted traffic performance from a GNN-MLP model with socioeconomic vulnerability of surrounding communities to quantified flood impacts on 18 highways and examined how integrating social vulnerability can shift recovery priorities across highway groups with different travel demand.

3 Methodology

The workflow of the methodology was structured in three parts as shown in Figure 1: (1) data collection (subsection 3.1); (2) GNN-based model for traffic prediction (subsection 3.2); and (3) dynamic impact indicator for flood assessments (subsection 3.3).

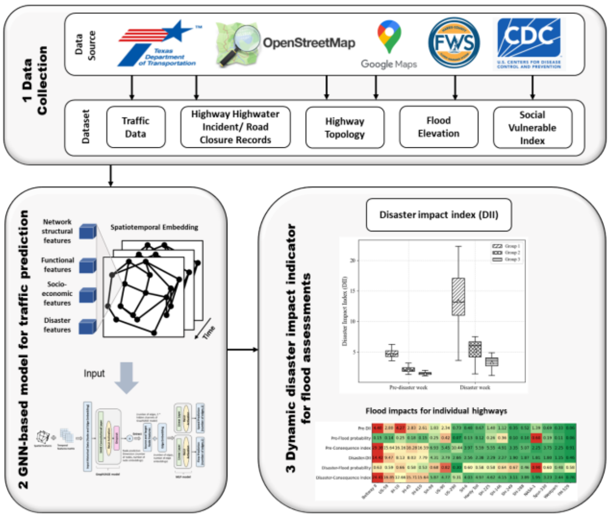

Figure 1. Workflow for flood impact assessment of highway networks

3.1 Data Collection

We collected four types of data: (1) network structural features, (2) functional features, (3) socio-economic features, and (4) disaster features. Table 2 introduces these data types, variables, and sources. flooding condition. Subsections 3.1.1-3.1.4 describe in detail the collection and processing of these four types of features. Section 3.1.5 introduces the road closures and network structure updates under the influence of floods.

Table 2 Input data types, variables, and sources

Date type	Variables	Data sources
Network structural features	Node degree centrality, node betweenness centrality, edge betweenness centrality	Texas Highway Freight Network [13]
Functional features	Traffic flow, traffic speed	Texas Department of Transportation [14], Houston TranStar [15]
Socio-economic features	Social vulnerability index	Centers for Disease Control and Prevention [16, 17]
Disaster features	Flood elevation,	Harris County Flood Warning System [18],

	flood probability	Texas Department of Transportation [14]

3.1.1 Network Structural Features

Network structural features capture the topological characteristics of the highway network, including node degree centrality, node betweenness centrality, and edge betweenness centrality. We collected the network structural features from the Texas Department of Transportation (TxDOT) and transformed them into a CSV format by manually identifying the node coordinates using Google Maps. We then constructed a directed graph $G = (V, E)$ with 546 nodes and 557 edges to encode the spatial topology of the highway network for subsequent spatiotemporal learning using GNN. Tensors $T_s \in \mathbb{R}^{J \times M_s}$ and $T_{ns} \in \mathbb{R}^{J \times N_s}$ represent the network structural features on the edges and nodes, respectively.

3.1.2 Functional Features

Functional features capture the functional performance of each highway segment, including traffic flow and speed. We collected the functional features from the TxDOT. Traffic flow data were later aggregated to characterize highway-level traffic demand and to support the classification of highways into different demand groups in the case study analysis. A speed value of zero can occur under two conditions: (1) a true zero, where a highway segment is closed, and no vehicle can pass; and (2) a false zero, where a highway segment is open, yet no vehicle travel through the segment during the recorded time. To reflect the actual condition, we kept the true zeros and used third-party speed data from Houston TranStar to supplement the false zeros. Tensor $T_f \in \mathbb{R}^{J \times M_f}$ represent the functional features on the edges.

3.1.3 Socio-economic Features

We used the social vulnerability index (SVI) to represent socio-economic features. The SVI data were collected from the Centers for Disease Control and Prevention (CDC) [17]. The SVI is the overall percentile rankings of 15 variables: below poverty, unemployed, income, no high school diploma, aged 65 or older, aged 17 or younger, civilian with a disability, single-parent households, minority, speak English "less than well," multi-unit structures, mobile homes, crowding, no vehicle, and group quarters. To integrate these data into the network, census-tract-level SVI values were mapped to graph nodes by assigning each node the SVI of the census tract in which it is located. This enables the representation of socio-economic vulnerability at the node level through the tensor $T_{sv} \in \mathbb{R}^{I \times N_{sv}}$.

3.1.4 Disaster Features

Disaster features used in this study were collected from the Harris County Warning System, including flood elevation and flood probability. The flood elevation is the water-surface elevation. Flood probability is an elevation threshold—when the water level reaches this height, it may cause flooding of surrounding roads. To map the disaster features on each highway segment, we first discretized the highway network into grids. Then, we mapped the flood elevation and flood probability from each monitoring station into these grids. Each highway segment was assigned the average value of the grids that it intersected. Tensors $T_d \in \mathbb{R}^{J \times M_d}$ represent the disaster features on the edges.

3.1.5 Road Closures and Network Structure Updates

We used the high-water incidents and road closures data provided by TxDOT to update the road network structure due to flooding. Each record contains the coordinates, detection time, and cleared time for each event. There are two flooding conditions of each grid: (1) flooded, with one or more flood or closure events; (2) unaffected, with no flood or closure event. Highway segments that intersected one or more flooding grids were marked as inundated. Accordingly, we updated the network structure based on the inundated segments.

3.2 GNN-Based Model for Traffic Prediction

We used a GNN model for generating node representations and a multi-layer perceptron (MLP) model for traffic prediction. We first conducted a rigorous hyperparameter selection to optimize six GNN-based variants and identify the most effective configuration based on root mean square error (RMSE), including GCN, STGCT, DCRNN, GAT, ChebNet and GraphSAGE. Then, we selected the GraphSAGE-MLP architecture for our case study, as shown in Figure 2.

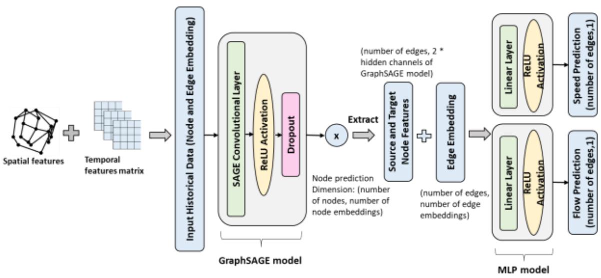

Figure 2 The architecture of the GraphSAGE-MLP case study model

Historical data, including node features (e.g., structural and social features) and edge features (e.g., disaster and functional features), is pre-processed as a spatiotemporal matrix and used as model input. First, node features are iteratively updated through neighbourhood aggregation in SAGE convolutional layers, followed by nonlinear regularization using the Corrected Linear Unit (ReLU) activation function and dropout to obtain node prediction results. Next, we extract the embedding vectors of source and target nodes and concatenate them with edge-specific features to generate comprehensive edge embedding vectors. These embedding vectors are then fed into an MLP model, where independent linear layers predict traffic speed and flow, respectively.

3.3 Dynamic Disaster Impact Indicator for Flood Assessment

We proposed a disaster impact indicator (DII) to assess the impact of floods, which can identify the highway segments most severely affected by floods. The concept of DII was proposed by Zhang et al. [19], referring to the probability of disaster occurrence and the consequences of segment disruption. To incorporate the real functional performance and the social influence from the surrounding vulnerable communities, we extended Zhang et al.'s definition by integrating functional and socio-economic features. The DII for a highway segment e is formulated as:

$$DII(e) = DP(e) \times CI(e) \tag{1}$$

where $DP(e)$ represents the probability of a highway segment e is flooded, derived from the disaster tensor $T_d \in R^{J \times M_d}$. $CI(e)$ refers to the consequence index, which measures the degree of disruption caused by highway segment e being flooded. The $CI(e)$ is defined as:

$$CI(e) = \frac{(S_i + S_j)}{2} \times F(e) \tag{2}$$

where S_i and S_j capture the social vulnerability at the starting and ending nodes of highway segment e, respectively. Both values are derived from the socio-economic feature tensor $T_{sv} \in R^{I \times N_{sv}}$. Specifically, S_i and S_j correspond to the SVI of the census tracts where node i and j are located. The functional feature $F(e)$ quantifies function performance road segment e, and is derived from the functional feature tensor $T_f \in R^{J \times M_f}$. The functional feature $F(e)$ is calculated as:

$$F(e) = \alpha F_f(e) + \beta F_s(e) \tag{3}$$

where traffic flow $F_f(e)$ and speed $F_s(e)$ are commonly-used indicators for evaluating functional performance. $F_f(e)$ characterizes the traffic-carrying capability of a highway, while $F_s(e)$ indicates its service quality. We normalized $F_f(e)$ and $F_s(e)$ to the range [0,1] to eliminate scale-related bias. The weighting parameters α and β, each ranging from 0 to 1, specify the relative emphasis placed on flow versus speed and can be adjusted according to analytical needs.

4 Case Study

We applied the proposed DII to assess flood impacts on the Harris County highway network during Hurricane Harvey from August 25 -31, 2017. Figure 4 shows the 18 highways within the study area, each highlighted with a distinct colour. To facilitate comparative analysis, these highways were grouped by their traffic demand calculated as the total traffic flows during the study period.

- Group 1 (high-traffic-demand) highways: IH-10, Beltway 8, US-59, IH-45, IH-610, and US-290.
- Group 2 (medium-traffic-demand) highways: SH-99, SH-225, Hardy Toll Road, SH-146, SH-288, and SH-249.
- Group 3 (low-traffic-demand) highways: Spur-330, SH-6, US-90, NASA-1, Westpark Tollway, and FM-529.

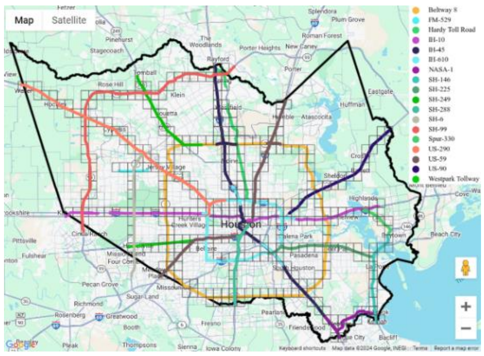

Figure 4 18 highways within the study area

4.1 Data Collection

Network structural, functional, socio-economic, and disaster features were collected and processed as introduced in Section 3.1. The dataset spans the period from August 18 to 31, 2017, with a temporal resolution of 15 minutes. Specifically, data from the pre-disaster period (August 18–24) and the initial phase of the disaster (August 25–27) were used as inputs to predict traffic conditions and flood impacts during the subsequent four days (August 28–31). In addition, high-water incidents and road closures were used to update the highway network structure during the flood.

4.2 GNN-Based Model for Traffic Prediction

We used the GraphSAEG-MLP model introduced in

Section 3.2 to predict the traffic flow and traffic speed. The model was trained using historical data from Aug. 18–27 to predict traffic conditions during Aug. 28–31, with approximately 71% of the data used for training and 29% for testing. The model was optimized using the Adam optimizer with a learning rate of 0.0001. Hyperparameter tuning was conducted for key model components, including the number of epochs, GraphSAGE layers, hidden channels, and dropout rate. The final model configuration consisted of 25 training epochs, 1 GraphSAGE layer, 16 hidden channels, and a dropout rate of 0.3.

The RMSE values of traffic prediction for each model were presented by a pair of box plots, where speed was represented in blue and flow was represented in red (Figure 3). The lines inside the box plots mark the median RMSE, and the green triangles represent the mean values. The y-axis was capped at 1.7 to enhance readability by preventing GraphSAGE-LSTM-MLP's outliers (exceeding 2.4) from distorting the scale. We found that GraphSAGE-MLP exhibited the lowest RMSE values for both traffic speed and flow with a compact interquartile range, indicating both high accuracy and low variance.

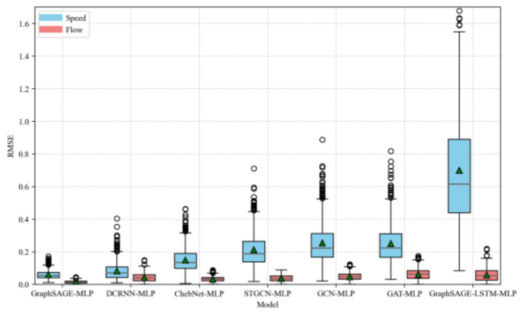

Figure 3 RMSE distribution for predicted speed and flow across models

4.3 Dynamic Disaster Impact Indicator for Flood Assessment

We calculated the DII for the pre-disaster week (August 18–24) using observed traffic data as a baseline. During the disaster week (August 25–31), observed data were used for the early disaster stages (August 25–27), while GNN-predicted traffic data were incorporated to assess flood impacts for subsequent periods (August 28–31).

First, we compared the DII across the three highway groups to evaluate how disaster impacts vary with traffic-demand levels. Second, we examined individual highways by their flood probability, consequence index, and DII to identify highways with high flooding probability, high disruption consequence, or both. Third, we explored how socioeconomic vulnerability affects flood impacts for highways with different traffic demand levels.

Figure 4 shows the boxplots of the DII across the three highway demand groups. Compared with the pre-disaster week, all groups experienced an expansion of the interquartile range (IQR) during the disaster week, indicating greater variability in impact severity among individual highway segments within the same group. Group 1 (high-traffic-demand) highways exhibited the largest DII values during the disaster, with a mean increase of 186.45%, indicating that suffered the most severe disruptions. This pattern aligns with most high-water events observed along these highways, highlighting the direct impact of flooding on them. In contrast, Group 3 (low-traffic-demand) highways showed the lowest DII values and the smallest relative increase from pre-disaster week (115.87%), implying relatively limited direct exposure to flooding. Examination of high-water records further indicates that the observed impacts on these highways were largely indirect, driven by suppressed travel demand in adjacent areas and reduced upstream network connectivity.

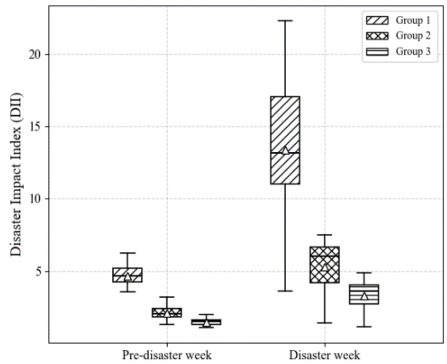

Figure 4 DII for pre-disaster week and disaster week by highway groups

We visualized the average flood probability, consequence index, and DII values of each highway during the pre-disaster and disaster weeks as a heatmap (Figure 5) to further examine the varying impacts of flood. These three indicators respectively capture a highway's exposure to flooding, its potential to disrupt network-wide mobility, and its overall disaster impact. As shown in Figure 5, highways are ranked in descending order of their DII values during the disaster week. Each row is colour-scaled independently—red indicating higher values and green indicating lower—to facilitate visual comparison.

The results revealed that highways such as Beltway 8, IH-10, and IH-45 already had high DIIs before the disaster, suggesting they are particularly vulnerable to potential impacts even before the flood. This is due to their locations in flood-prone (Beltway 8) or low-lying areas (IH-45) and their critical roles in regional traffic

(IH-10). This result highlights the need for flood prevention infrastructure and pre-disaster traffic management plans for these highways. Beltway 8, US-59, and IH-10 exhibited the highest DIIs during the disaster, indicating that these highways experience the most significant impacts during the flood. This underscores the need to prioritize these highways in disaster response and recovery, including timely road clearance and emergency access restoration to minimize cascading network disruptions.

Interestingly, despite having the lowest flood probability during the disaster (only 0.3), US-290 showed relatively high DII and consequence index values. This is likely because US-290's strategic location as a connector between high-traffic regions makes it vulnerable to network-level disruptions, even under minor local flooding. This result highlights that flood probability alone does not determine impact severity. Therefore, disaster preparedness and resilience planning should place greater emphasis on the potential consequences of disruptions.

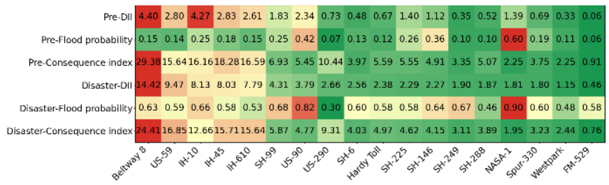

Figure 5 Average flood probability, consequence index, and DII for each highway during pre-disaster and disaster weeks

To quantify the influence of incorporating socio-economic vulnerable features, DII-based highway rankings during the disaster week were examined with and without the inclusion of SVI (Figure 6). The horizontal axis uses distinct font colours to denote highway demand groups, with blue, orange, and green representing Groups 1, 2, and 3, respectively. In both cases, Group 1 (high-traffic-demand) highways consistently had the highest DII, confirming the robustness of the overall priority. However, noticeable ranking shifts were observed among Group 2 (medium-traffic-demand) and Group 3 (low-traffic-demand) highways. Within Group 2, most highways experienced a decline in ranking after incorporating SVI, with only a few exceptions, such as SH-225 and SH-288, showing improvements. In contrast, Group 3 highways exhibited more pronounced heterogeneity. For instance, NASA-1 experienced a substantial drop in ranking, whereas US-90 and SH-6 rose by three positions, indicating that certain low-demand highways gained priority when socio-economic vulnerability was considered.

This pattern suggests that incorporating socio-economic vulnerability does not merely reshape rankings within individual demand groups but instead induces a cross-group reallocation of recovery priority. Specifically, priority shifts away from medium-demand highways toward low-demand highways that serve more socially vulnerable communities. This highlights that equity considerations can elevate the importance of otherwise lower-demand infrastructure when their surrounding populations are more vulnerable. From a broader perspective, these findings indicate that socio-economic features introduce a redistribution mechanism in recovery prioritization, moving beyond efficiency-driven decisions based solely on traffic demand. In practice, this implies that planners should pay attention to low-demand highways that may serve vulnerable communities, as they can become critical candidates for earlier intervention despite their lower functional prominence.

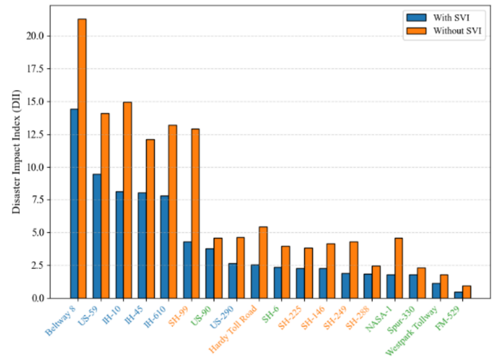

Figure 6 Highway DII rankings with and without SVI during the disaster week

5 Conclusions

This study proposed a DII that integrates predicted traffic performance with surrounding socioeconomic vulnerability to quantitatively assess the impacts of floods on highway networks. We first collected four types of features and then fed them into a GraphSAGE-MLP model for traffic prediction. Subsequently, the DII was calculated using the predicted traffic flow data. Using the flooding caused by Hurricane Harvey in Harris County as a case study, we quantified the impact of the flood on individual highways and demonstrated how socioeconomic vulnerability influences the flood impact on highway groups with different travel demands.

Several key findings emerge from this study. First, high-traffic-demand highways are more severely affected by floods. Second, assessing flood impact requires considering not only flood probability but also the consequences of the damage. Third, incorporating socio-economic features preserved the identification of critical highways while refining the prioritization of medium-traffic-demand highways to emphasize highways that serve socially vulnerable communities.

The academic contributions of this study are (1) developing a unified DII that captures network structural, functional, and socioeconomic features to assess flood impacts; (2) investigating how socioeconomic vulnerability shapes recovery prioritization across traffic-demand groups. However, this study has some limitations. First, the analysis relies on data spanning only one week before and one week during the flood. Second, the SVI employed in this study is static and does not capture potential temporal variations in social conditions or behavioral responses throughout the disaster period. Future work could incorporate dynamic social indicators (e.g., mobility data) to better represent evolving population behavior and vulnerability during disaster events, thereby improving the realism of recovery prioritization.

References

[1] M. Diakakis, N. Boufidis, J. M. S. Grau, E. Andreadakis, and I. Stamos, “A systematic assessment of the effects of extreme flash floods on transportation infrastructure and circulation: The example of the 2017 Mandra flood,” *International journal of disaster risk reduction,* vol. 47, pp. 101542, 2020.

[2] B. Dong, S. Ding, L. Wu, and X. Li, “Short-term natural disaster impacts on transportation infrastructure: a systematic review,” *Natural Hazards*, pp. 1-42, 2025.

[3] Y. Chen, Q. Wang, and W. Ji, “Rapid assessment of disaster impacts on highways using social media,” *Journal of Management in Engineering,* vol. 36, no. 5, pp. 04020068, 2020.

[4] A. Gori, I. Gidaris, J. R. Elliott, J. Padgett, K. Loughran, P. Bedient, P. Panakkal, and A. Juan, “Accessibility and recovery assessment of Houston’s roadway network due to fluvial flooding during Hurricane Harvey,” *Natural hazards review,* vol. 21, no. 2, pp. 04020005, 2020.

[5] M. Zamanifar, and T. Hartmann, “Decision attributes for disaster recovery planning of transportation networks; A case study,” *Transportation research part D: transport and environment,* vol. 93, pp. 102771, 2021.

[6] V. S. Harandi, K. A. Hosseini, and B. Mansouri, “Assessing the effect of physical and social parameters on seismic risk of urban transportation networks,” *International Journal of Disaster Risk Reduction,* vol. 101, pp. 104269, 2024.

[7] E. Merschman, M. Doustmohammadi, A. M. Salman, and M. Anderson, “Post-disaster decision-making framework for roadway networks considering social vulnerability,” *Travel Behaviour and Society,* vol. 38, pp. 100910, 2025.

[8] J. Yin, D. Yu, Z. Yin, M. Liu, and Q. He, “Evaluating the impact and risk of pluvial flash flood on intra-urban road network: A case study in the city center of Shanghai, China,” *Journal of hydrology,* vol. 537, pp. 138-145, 2016.

[9] O. Woolley-Meza, D. Grady, C. Thiemann, J. P. Bagrow, and D. Brockmann, “Eyjafjallajökull and 9/11: The Impact of Large-Scale Disasters on Worldwide Mobility,” *PLoS ONE,* vol. 8, no. 8, 2013.

[10] M. Pregnolato, A. Ford, S. M. Wilkinson, and R. J. Dawson, “The impact of flooding on road transport: A depth-disruption function,” *Transportation research part D: transport and environment,* vol. 55, pp. 67-81, 2017.

[11] H. A. Elfenbein, “7 Emotion in organizations: a review and theoretical integration,” *Academy of management annals,* vol. 1, no. 1, pp. 315-386, 2007.

[12] A. Alipour, and B. Shafei, “Assessment of Postearthquake Losses in a Network of Aging Bridges,” *Journal of Infrastructure Systems,* vol. 22, no. 2, pp. 12, Jun, 2016.

[13] Texas Department of Transportation. "TxDOT Texas Highway Freight Network," 12/09/2024.

[14] Texas Department of Transportation. 06/21/2024, 2024; https://www.txdot.gov/.

[15] Houston TranStar. 10/16/2024, 2024; https://traffic.houstontranstar.org/speedcharts/.

[16] Centers for Disease Control and Prevention. "CDC’s Social Vulnerability Index (SVI) – 2016 overall SVI, census tract level," 08/01/2024, 2024; https://www.arcgis.com/home/item.html?id=62b3e305b730423782c64b9696242c5e#overview.

[17] Centers for Disease Control and Prevention. "CDC Social Vulnerability Index 2018 - USA," 08/01/2024, 2018; https://www.arcgis.com/home/item.html?id=cbd68d9887574a10bc89ea4efe2b8087.

[18] Harris County Flood Warning System. 09/23/2024, 2024; https://www.harriscountyfws.org/.

[19] Q. Zhang, H. Yu, Z. Li, G. Zhang, and D. T. Ma, “Assessing potential likelihood and impacts of landslides on transportation network vulnerability,” *Transportation research part D: transport and environment,* vol. 82, pp. 102304, 2020.